Automatic Identification of Grey Matter Structures from MRI to Improve the Segmentation of White Matter Lesions

Simon Warfield* Joachim Dengler† Joachim Zaers‡ Charles R.G. Guttmann§
William M. Wells III¶ Gil J. Ettinger‖ John Hiller** Ron Kikinis††

Abstract

The segmentation of MRI scans of patients with white matter lesions (WML) is difficult because the MRI characteristics of white matter lesions are similar to those of grey matter. Intensity based statistical classification techniques misclassify some WML as grey matter and some grey matter as WML.

We developed a fast elastic matching algorithm that warps a reference data set containing information about the location of the grey matter into the approximate shape of the patient's brain. The region of white matter was segmented after segmenting the cortex and deep grey matter structures. The cortex was identified using a 3D region growing algorithm constrained by anatomical, intensity gradient and tissue class parameters. White matter and white matter lesions were then segmented without interference from grey matter using a two class minimum distance classifier.

Analysis of double echo spin echo MRI scans of sixteen patients with clinically determined multiple sclerosis (MS) was carried out. The segmentation of the cortex and deep grey matter structures provides anatomical context. This was found to improve the segmentation of MS lesions by allowing correct classification of the white matter region despite the overlapping tissue class distributions of grey matter and MS lesion.

1 Introduction

The segmentation of MRI scans of patients with white matter lesions is difficult because the MRI characteristics of white matter lesions (WML) are similar to those of grey matter. Intensity based statistical classification techniques misclassify some WML as grey matter and some grey matter as WML. We developed a technique to identify a mask of the white matter region of the brain. White matter and white matter lesions were then segmented without interference from grey matter.

The use of MRI for monitoring of treatment trials in MS has been analyzed.[9] The characterization of MS requires long term serial studies (typically 1-2 years) because of the relatively slow progression of the disease. MRI scans with thin contiguous slices are desirable, with scanning repeated at intervals of 1-3 months. Quantitative assessment of the appearance of high intensity regions in MRI scans is important to evaluate the disease activity and progression.[12] Manual analysis of this volume of data is expensive and tedious. The intra- and inter-rater reliability of semi-automatic methods of analysis range from 5-20%.[9] The requirements to reduce human interaction (in order to improve reproducibility and to derive a measure of lesion burden that is independent of the operator) and to improve the accuracy of lesion load measurements were identified as important goals for any new segmentation methods in a recent review.[4] However, automatic segmentation is difficult because of the similarity of the pixel intensity of MS lesions and grey matter.

Attempts have been made to deal with the overlapping intensity range of normal grey matter and lesion tissue. One approach used a model involving a spatially varying prior probability density for brain tissue class.[7] The search for MS lesions was confined to those regions with at least a 50% prior probability of being white matter. In this way, the incorrect classification of grey matter as MS lesion was greatly reduced. This model compensates for the tissue class intensity overlap by using a probabilistic model of the location of MS lesions. Our method segments the white matter region from each scan, rather than using a probabilistic model for

*simonw@bwh.harvard.edu. Journal Image Guided Surgery, Vol. 1, Num. 6, pp.326–338, 1995, and at http://journals.wiley.com/cas/v1n6/95042-intro.html

†Vision Systems, Neckargemuend, Germany, nuk111@cvx12.inet.dkfz-heidelberg.de

‡DKFZ (German Cancer Research Center) D-69120 Heidelberg Germany, J.Zaers@dkfz-heidelberg.de

§Harvard Medical School and Brigham and Women's Hospital, Department of Radiology, 75 Francis St., Boston, MA 02115, guttmann@bwh.harvard.edu

¶Harvard Medical School and Brigham and Women's Hospital, Department of Radiology, 75 Francis St., Boston, MA 02115, sw@bwh.harvard.edu

‖AI Lab NE43-771, Massachusetts Institute of Technology, 545 Technology Square, Cambridge MA 02139, ettinger@ai.mit.edu

**UCLA School of Medicine, Department of Radiological Sciences, hiller@endeavor.radsci.ucla.edu

††Harvard Medical School and Brigham and Women's Hospital, Department of Radiology, 75 Francis St., Boston, MA 02115, kikinis@bwh.harvard.edu

all scans, and is able to correct both grey matter as MS lesion and MS lesion as grey matter classification errors.

Another approach is to use a combination of interactive manual intervention and statistical classification.[11] A trained operator interactively selects locations inside a lesion, and then k-NN classification and connected component labelling are used to segment the lesion. This process is repeated until the operator is satisfied with the segmentation of the lesion. The analysis procedure is repeated for each lesion to be segmented. Incorrect classification caused by overlapping pixel intensities is avoided by having the operator interactively correct the classification. The operator uses knowledge of normal brain anatomy in order to differentiate between MS lesion and other brain tissue.

One approach to incorporating knowledge of normal brain anatomy automatically is to regard the segmentation of the brain as a registration problem. An atlas containing a description of normal brain anatomy is registered to a patient data set using a rigid transformation. Local shape difference between the patient and the atlas are then resolved using local elastic deformations. This technique has been used to achieve robust segmentation of sub-structures of the brain.[1] Patient data sets were registered to an average brain volume, and a polyhedral model of important brain structures used to identify anatomical structures.

Elastic matching algorithms are not able to segment structures in the patient that are not present in the atlas, such as white matter lesions. Unlike some brain tumours, MS lesions do not cause significant distortion of a patient's anatomy. Elastic matching may be unable to compensate for the distortion caused by a tumour, because the difference between the atlas and patient brain structure shape is not well described by an elastic deformation. The normal anatomical variability of the cortex is also not well described by an elastic deformation.

We have developed a segmentation method that uses the positive features of both statistical classification and elastic matching methods to overcome the limitations present when the techniques are used alone. Our method is a general method which uses anatomical information to disambiguate the segmentation when class distributions overlap in feature space. This approach is well suited to the segmentation of MRI scans of MS patients because of the substantial degree of overlap of the MS lesion class with other tissue classes (particularly grey matter). It is a new automatic method that produces a segmentation that is superior to that possible with either elastic matching or statistical classification alone.

The principal results of this study are an algorithm for the automatic segmentation of the cortex, a method for the automatic identification of the region of white matter and a method for the segmentation of WML. This method has been applied to MRI scans of sixteen patients with clinically determined MS and to scans with simulated lesions. Together these indicate that the method accounts for the ambiguity due to the overlapping intensity distributions of grey matter and WML, and consequently improves the segmentation of these tissue classes.

2 Description of Method

Motivation

A major difficulty for accurate segmentation of WML is the overlapping intensity distributions of WML and grey matter. Some regions of lesion cannot be distinguished from grey matter and vice versa even when powerful nonparametric multispectral statistical classification techniques are used. Some lesions have intensity characteristics entirely in the range of that of grey matter, with no voxel having an unambiguous lesion intensity. They can be recognized as lesion by an experienced observer as they appear in the region of the white matter where no grey matter is expected. The segmentation must be done in 3D since 2D slices can show small blobs of cortex which appear to be white matter lesions. In a slice these appear isolated, but examination of neighbouring slices shows that they are connected to the cortical mantle.

The same problem manifests itself in another form. The typical slice thickness used in MS studies with double echo spin echo MRI gives rise to significant partial volume artifacts. The relatively low spatial resolution of these scans gives rise to boundaries between different tissue types that are difficult to distinguish. This occurs particularly at the edge of the brain, where cerebrospinal fluid (CSF) and grey matter are averaged together. This sometimes causes voxels to have a pixel intensity range typical of MS lesion. Any intensity based statistical classifier will misclassify such voxels as MS lesion.

If it is assumed that MS lesions always occur within white matter then we can differentiate between MS lesions in white matter and other voxels with pixel intensities similar to MS lesions using our new segmentation algorithm.

Segmentation Algorithm Overview

The segmentation algorithm is represented schematically in Figure 1. The primary input to the segmentation process is a double echo spin echo MRI scan of a patient. The MRI scan is smoothed to improve SNR and the intracranial cavity is segmented. Classification and intensity inhomogeneity correction is carried out with the Expectation-Maximization algorithm. Our atlas is first aligned to the patient scan with a six parameter (three translation and three rotation) linear transformation, and then local shape differences are resolved with our elastic matching algorithm. The deep grey matter structures are segmented directly by elastic matching. However, the normal anatomical variability of the grey matter of the neocortex is not well described by an elastic deformation. Consequently, a new 3D constrained region growing algorithm was developed in order to segment the cortex. After the grey matter structures have been segmented using these algorithms, the white matter region is segmented and reclassified into white matter and WML classes. This process re-

solves the ambiguity caused by the overlapping intensity distributions of the grey matter and WML classes.

Contrast Preserving Noise Smoothing

Edge preserving noise smoothing is carried out on the scan by iteratively solving the nonlinear diffusion equation

$$\frac{\partial I}{\partial t} = \nabla \cdot (c \nabla I)$$

where I is the vector-valued MRI scan, t is time (iteration number), $c = \frac{1}{1+\left(\frac{|\nabla I|}{\kappa}\right)^2}$ is the spatially varying conductance function and κ is the noise strength parameter.[5] Since the in-plane resolution of our scans (0.9375mm) is much smaller than the thickness of the slices (3mm), the conductance across the slices of the scans is negligible. It has been shown that the use of nonlinear diffusion filtering reduces the variability of operator-guided segmentation of MS lesions acquired with 1.5 T MRI exams.[10]

Intracranial Cavity Segmentation

The intracranial cavity (ICC) is segmented using a semi-automatic method.[8] A parzen window classifier is used to segment the volume into brain and non-brain classes. Some material outside the ICC is still classified as brain, so 3D erosion followed by supervised connectivity analysis and 3D dilation is performed. The resulting binary data set represents the region of the intracranial cavity. This is the only processing step that requires manual interaction for each patient volume. The interrater reliability has been assessed and the standard deviation of the area of the ICC segmentation was found to be 0.5%.[8] The ICC mask is used for the calculation of the linear registration and to exclude material external to the brain from the later processing steps.

Classification and Intensity Inhomogeneity Correction

Intensity-based statistical classification and intensity inhomogeneity correction are calculated simultaneously using the Expectation-Maximization (EM) segmentation algorithm.[17] The EM segmenter generates two data sets for each patient data set. These are the statistical classification of each voxel and the value of the DE SE MRI after correction for the intensity inhomogeneity. Automatic correction of intensity inhomogeneity in this way makes the segmentation robust against minor changes in MR operating characteristics as well as correcting for the inherent intensity inhomogeneity (shading artifact). Consequently, it is possible to carry out supervised classification on one patient scan and to use the same statistical model for the distribution of tissue classes to segment other scans of the same acquisition type. There is no need to retrain the classifier. This algorithm is run fully automatically, without any user intervention, on each noise smoothed patient scan.

The algorithm proceeds by iteratively estimating the tissue class and intensity inhomogeneity at each voxel, until both estimates have converged. The intensity inhomogeneity is modelled as an additive bias field in a log-transformed data set and is estimated by solving

$$\hat{\beta} \leftarrow H(Y - WU)$$

where $\hat{\beta}$ is a vector representing the bias field, H is a low pass filter, Y is a vector of the observed tissue intensities (image pixel values), $U = (\mu(c_1), \mu(c_2), \ldots)$ is a vector of the mean intensity of each tissue class, c_k represents tissue class k and W is a matrix of a posteriori tissue class probabilities (weights used to predict the signal intensity).

The distribution of observed pixel values for a single channel data set is modelled by

$$p(Y_i|\Gamma_i, \beta_i) = G_\sigma(Y_i - \mu(\Gamma_i) - \beta_i)$$

where $G_\sigma(x)$ is a zero mean Gaussian distribution with variance σ^2, and the tissue probability (weight) matrix W_{ij} can be estimated by

$$W_{ij} \leftarrow \frac{P(c_j)p(Y_i|c_j, \hat{\beta}_i)}{\Sigma_{\Gamma_i} P(\Gamma_i)p(Y_i|\Gamma_i, \hat{\beta}_i)}$$

where $P(c_j)$ is the a priori probability of tissue class c_j. Voxel i is classified by selecting the class for which W_{ij} is largest.

Linear Registration

A linear transformation (with three translation and three rotation parameters) is computed in order to align the ICC of the atlas with that of the patient. The goal of the linear registration is to compute a global alignment of the atlas and patient data sets so that the elastic matching algorithm that follows can successfully deform the atlas to account for local shape differences. The linear transformation is computed by minimizing the distance between the surfaces of the ICCs.

The voxels at the surface of the ICC for the atlas and patient are segmented. For each slice, the largest connected component of the background is found and the voxels of the ICC adjacent to this are identified as the surface voxels. The linear transformation T is found by using Powell's method to minimize

$$\sum_i \min\left(d_{max}^2, \min_j |T a_i - p_j|\right)$$

where a_i are the atlas surface voxels, p_j are the patient surface voxels and d_{max} is a maximum distance threshold to limit the contribution any single voxel can make. The RMS error in the match obtained with this method is of the order of the voxel size.[3]

Elastic Matching

A 3D volumetric reference data set (atlas) is matched to the anatomy of the patient in order to provide a segmentation of the normal anatomy. Our anatomical atlas was constructed by a combination of statistical classification and manual labelling of every voxel in a 3D SPGR MRI scan of a normal volunteer. It consists of both a grey scale data set and a labelled data set.[16] The purpose of the atlas is to describe normal brain anatomy for a specific person in such a way that the atlas labels can be transferred to another person's anatomy, without the need to repeat the arduous and time-consuming hand labelling that was required to construct the atlas. We have developed a fast and effective elastic matching algorithm by which the atlas labels can be transferred automatically to another data set.[2]

The nonlinear transformation relating the atlas anatomy to the patient anatomy is modelled as a 3D deformation field. Estimation of the local displacement vector $U = (u, v, w)^T = U(x, y, z)$ can be formulated as a standard regularization problem.[14] The deformation is determined by minimizing

$$E(U) = \iiint P(U) + \lambda D(U)\, dx\, dy\, dz$$

This functional describes a balance between the deformation energy $D(U)$ and local similarity of the images $P(U)$ as a function of the deformation. The local similarity $P(U)$ is determined by binary correlation of the atlas and patient segmented data sets over a small neighbourhood. The deformation energy term $D(U)$ is based on a physical model of a 3D elastic membrane, and is independent of the data. This is

$$D(U) = u_x^2 + u_y^2 + u_z^2 + v_x^2 + v_y^2 + v_z^2 + w_x^2 + w_y^2 + w_z^2$$

Applying a finite element discretization leads to linear Euler-Lagrange equations corresponding to the functional. This system of equations can be efficiently solved using a nested multigrid algorithm with conjugate gradient relaxation.[15]

The deformation field is calculated in two stages. Initially it is assumed to be flat. U is estimated on the basis of the brain parenchyma (grey matter and white matter and for the purpose of matching, WML is treated as white matter). This is done by solving for U using binary data sets corresponding to the brain parenchyma from the atlas labels and from the classified patient data set. The deformation field obtained is then used as the initial deformation and the estimate is refined by repeating the matching procedure using binary data sets corresponding to only white matter.

Brain structures that have a regular and consistent shape across many people, such as the deep grey matter structures of the diencephalon and telencephalon, and the cerebellum are directly segmented. Some deep grey matter structures (particularly the globus pallidus) can have an intensity characteristic similar to that of white matter, and so are misclassified by intensity based statistical classification. Elastic matching provides robust and accurate localization of these structures.

However, the variation of the shape of the cortex between different people is not well described by an elastic deformation. The atlas represents the anatomy of one normal volunteer. The normal anatomical variability of the cortex can mean that a patient has a gyrus where the atlas has none, or vice versa. When elastic matching is carried out, the region of the cortex is recovered, but precise localization of the borders of the cortex is not achieved.

Segmentation of the Cortex

Segmentation of the cortex has not been achieved using either statistical classification or elastic matching techniques alone. Statistical classification is able to identify the grey matter that makes up the cortex, but not to differentiate between the cortex and other grey matter structures. Elastic matching provides an estimate of the region of the cortex, but not a precise localization of the boundary of the cortex.

We have developed a new algorithm for segmentation of the cortex with a constrained 3D region growing algorithm. The algorithm uses the anatomical information provided in the atlas, tissue class information from statistical classification, the data intensity gradient and a simple model of the structure of the cortex.

Model of the cortex

We assume that the cortex has the form of a thick "blanket" crumpled over itself. One edge of the cortex, the outer edge, is adjacent to CSF. There exists a path joining every pair of voxels in the cortex that passes only through voxels of the cortex. Therefore, it is possible for a region growing algorithm to segment the cortex. It is necessary to consider the structure of the cortex in 3D, since in 2D slices parts of the cortex may appear to be disconnected from other parts.

Selection of cortex seed voxels

The region growing algorithm is started from seed locations automatically identified at the outer edge of the cortex. The region outside the ICC is masked out of the classified MRI data set and CSF is removed by relabelling it as background. At the outer boundary of the cortex there is often a layer of misclassified voxels, caused by partial volume averaging of the brain and CSF. This is removed by performing erosion on each slice of the classified data set with a 3x3 circular structuring element. Voxels on the outer surface of the brain are identified with the same algorithm that is used to identify the surface of the ICC for linear registration. The atlas labels are used to identify and eliminate voxels that are outside the region of the cortex. The location of each voxel identified is then used as a seed location for the region growing.

Anatomical constraint

The elastic match of the atlas to the cortex provides a good estimate of the region of the cortex but doesn't accurately localize the borders of the cortex. A region that includes the borders of the cortex is generated by 3D dilation of the matched cortex. This new region forms a mask that is used to restrict the range over which region growing is carried out. The mask represents an estimate of the maximum error that is possible in the elastic match of the cortex.

The deep grey matter structures and the cerebellum, as determined by the elastic match, are masked out so that these structures can't be incorrectly included in the cortex region.

Tissue intensity constraint

The cortex is a structure of grey matter. Only voxels with the pixel intensity range of grey matter, as determined with the EM segmentation algorithm, are considered. Partial volume averaging artifacts are corrected by relabelling after the cortex is segmented.

Tissue gradient constraint

White matter lesions can appear as a bright centre region with a dimmer "halo" surrounding it and also as a bright rim surrounding a darker centre.[6] This implies that there is a significant rate of change of intensity as we move out from the centre of a lesion. A high rate of change of pixel intensity is indicative of an edge in the image. An edge is found by locating local maxima of the gradient after smoothing with nonlinear diffusion.[13] The region growing process is not allowed to cross an edge. This constraint is implemented by constructing a binary volume in which voxels are set if an edge is indicated, and are not set in the absence of an edge. This constraint is used so that the region will not be able to grow from the cortex region to voxels around a lesion if there is an intensity gradient present.

Cortex Segmentation Region Growing Algorithm

The location of each seed voxel is placed in a queue and marked in a binary volume representing the cortex. Region growing proceeds by applying the following until the queue is empty, creating a binary volume representing the segmentation of the cortex.

```
Take location v from head of queue,
For each l in the neighbourhood of v,
    if (l is not marked as cortex) and
    if (l is in the cortex mask) and
    if (l has grey matter class) and
    if (l is not at a peak in the intensity gradient) then
            mark l as cortex
            add l to the queue
```

Segmentation of the White Matter Region

The white matter region consists of those voxels in the brain MRI scan that are healthy or diseased white matter (lesion). Some of these voxels are incorrectly classified as grey matter because the pixel intensity of the white matter lesion class and the grey matter class overlap. The combination of elastic matching and the cortex segmentation algorithm allow us to segment the grey matter of the brain.

Partial volume averaging causes some grey matter to be incorrectly classified as white matter lesion. This error is particularly severe in the slices at the top of the brain and around the cerebellum. The regions at the boundary between the cortex and CSF which are classified as lesion due to partial volume averaging are corrected by relabelling these regions as grey matter.

The white matter region is then segmented. The white matter region is the region inside the intracranial cavity, less those voxels identified as CSF, less those voxels segmented directly by elastic matching, less those voxels identified as cortex.

Segmentation of White Matter Lesions

Some voxels in the white matter region are erroneously classified as grey matter by the EM segmenter because of the overlapping intensity range of the grey matter and the white matter lesion classes. Voxels in this region should be classified only as white matter or as white matter lesion. Each voxel in the region is reclassified as either white matter or as white matter lesion using a two class two channel minimum distance classifier.

3 Results

Double echo spin echo MRI scans of sixteen patients with clinically determined multiple sclerosis were acquired on a GE Signa 1.5T clinical scanner with TR/TE_1/TE_2 3000/30/80 ms, FOV 24cm and contiguous 3mm thick axial slices covering the entire brain.

The segmentation process was applied to each MRI scan. The segmented data sets were then analysed to assess the consistency and accuracy of the segmentation of the cortex and MS lesions.

The EM segmentation algorithm and rigid registration each required about one hour to execute on each scan, running on a Sun SPARCstation 20/612. The 3D elastic deformation was calculated on an IBM RS/6000 workstation. The calculation required about 7 minutes to project the 3D volumetric atlas data set onto a MS patient data set. The accuracy of the match was improved by iterating the elastic match procedure 5 times. The cortex and lesion segmentation required about 30 minutes per scan on a Sun SPARCstation 20/612. The segmentation of a typical data set required about 3 hours overall.

To assess the effectiveness of our cortex segmentation algorithm, we compared the segmentation with the segmen-

	Rater A	Rater B	Rater C	Rater D	Rater E	automatic
agreement	96.9	93.6	94.4	95.0	88.8	95.2

Table 1: Comparison of rater performance with "standard" segmentation of the cortex in one slice. Agreement is measured as the percentage of voxels correctly segmented — $100(\frac{\#(S \cap C)}{\#C})$ where S is a segmentation and C is the "standard" segmentation formed by selecting those voxels that at least 5 of the 6 segmentations agree were cortex.

tation of five different raters. The cortex was segmented once by five different raters and by our automatic analysis method. The raters "painted" the region of the cortex on the same slice of one patient scan. Since the true segmentation of the cortex is unknown, a "standard" segmentation of the cortex for comparison was constructed by selecting those voxels that at least five of the six segmentations agreed were in the cortex. The agreement of a segmentation with the standard cortex segmentation was measured as the percentage of voxels of the standard cortex correctly segmented. Table 1 shows the agreement of the rater segmentations and the automatic segmentation with that of the "standard" cortex segmentation.

Figure 2(a) illustrates the variation in segmentation that different raters produce. Figure 2(e) shows the region selected as the standard cortex segmentation. The segmentations of different raters are consistent in the labelling of the centre region of the cortical grey matter, but vary in determining the inner and outer boundary of the cortex. This result is consistent with the observation that structures with a complex boundary shape are more difficult for people to segment than structures with a simple boundary.[8] People have a tendency to over- or under-estimate the boundary, as compared to an automatic segmentation. Consequently, manual segmentation exhibits a consistent variability in the segmentation of voxels at the boundary of cortical grey matter.

The segmentation of simulated data sets was carried out in order to evaluate the segmentation when the true segmentation is known. A lesion with a bright central region smoothly dimming towards the border was selected from one slice of a patient's MRI scan. Statistical classification of the lesion incorrectly segments it into a lesion component and a grey matter component. This lesion was inserted into the test slice and the entire scan was segmented. The segmentation of the lesion was found to vary with the lesion location. When the entire lesion was placed into the white matter it was segmented accurately. When the lesion was inserted into the cortex, the lesion was segmented as cortex — that is, the lesion appeared as a partial volume averaging artifact and so was labelled as cortex. When the lesion was placed partly in the cortex and partly in the white matter, all voxels with an unambiguous lesion intensity were segmented as lesion, some of the voxels (those in the white matter) were segmented as lesion and some were segmented as cortex. This is shown in Figure 3. The segmented tissue classes are, in order of decreasing intensity, white matter, white matter lesion, grey matter, CSF and background.

Figure 4 shows a typical result from our white matter lesion segmentation method applied to a patient with moderate lesion burden. The image shows the effectiveness of our method for correcting the misclassification apparent with statistical classification. The image shows that our new method improves the segmentation of both grey matter and MS lesion.

Figure 5 and Figure 6 illustrate the segmentation of lesions detected automatically for 16 patient data sets. These figures allow comparison of the difference between using statistical classification and our new method. They demonstrates that partial volume averaging artifacts appear as a large proportion of the voxels classified as lesion with statistical classification alone. Figure 7 is a magnified view of one pair of these images. The segmentation with the new method better delineates the white matter lesions, and does not have the partial volume averaging errors present in the EM segmentation. The two large lesions on the patient's left side are larger and a clear pattern of periventricular lesion can be seen. This is obscured in the EM segmentation because the EM segmenter misclassifies part of these lesions as grey matter.

4 Discussion and Conclusion

Intensity based statistical classification has been used to segment MRI scans into different tissue classes. However, when tissue class distributions overlap some voxels are misclassified. This makes the segmentation of MS lesions particularly difficult because the intensity distribution of MS lesions strongly overlaps other classes (especially grey matter) in double echo spin echo MRI.

We have developed a general method for automatically incorporating knowledge of normal brain anatomy into the segmentation process. This allows correct segmentation of different structures that have a similar pixel intensity range. Elastic matching can be used to segment subcortical structures directly. The segmentation achieved using elastic matching is also able to distinguish between different structures of the same tissue class. Elastic matching allows boundaries between structures not clearly resolved in MRI to be determined using the normal anatomy as a model. However, the elastic matching technique is not able to segment structures which are not present in the atlas, such as white matter lesions. The elastic deformation model has been able to match subcortical anatomy but has not yet proven able to model the normal anatomical variability exhibited by the cortex.

We have developed a new algorithm for the segmentation

of the cortex. Table 1 shows our new cortex segmentation algorithm produces a segmentation that is consistent with that of manual segmentation, and has better reproducibility since it produces the same segmentation each time it is repeated. We have developed a method for the identification of the region of the white matter in MRI scans of the brain. We have shown that this allows for improved segmentation of white matter lesions.

Segmentation of simulated lesions has indicated that MS lesions in the white matter can be accurately segmented, and that an explicit anatomical model can be used to identify and correct misclassification due to partial volume averaging.

Statistical classification exhibits two kinds of error which are corrected by our new method. The first is the incorrect classification of some voxels as white matter lesion, due to partial volume averaging and inherent class intensity distribution overlap. This error is corrected by relabelling voxels classified as lesion if they are outside the white matter region. The second is the incorrect classification of some lesion voxels as grey matter. This error is corrected by reclassifying the white matter region with a two class minimum distance classifier.

We are investigating the application of this method to the segmentation of scans of patients with brain tumours. In these scans the observed anatomy can be significantly distorted from that of the atlas. We are investigating the automatic determination of the anatomical location of each MS lesion by reference to the anatomical atlas. We are also investigating the use of our segmentation method to study the evolution of MS lesions over time.

Acknowledgements The authors gratefully acknowledge the assistance of Aybuke Aurum, Qi Chen and Wendy Harrison with the manual segmentation of the cortex, the assistance of Marianna Jakab in the preparation of the ICC masks, and the technical support provided by Adam Shostack, Mark Anderson and Aidan Williams.

References

1. Collins DL, Peters TM, Dai W, Evans AC (1992) Model based Segmentation of Individual Brain Structures from MRI Data. In SPIE Vol. 1808, Visualization in Biomedical Computing pp. 10–23.

2. Dengler J, Schmidt M (1988) The Dynamic Pyramid – A Model for Motion Analysis with Controlled Continuity. International Journal of Pattern Recognition and Artificial Intelligence 2(2):275–286.

3. Ettinger GJ, Grimson WEL, Lozano-Perez T, Wells III WM, White SJ, Kikinis R (1994) Automatic Registration for Multiple Sclerosis Change Detection. In IEEE Workshop on Biomedical Image Analysis.

4. Filippi M, Horsfield MA, Tofts PS, Barkhof F, Thompson AJ, Miller DH (1995) Quantitative assessment of MRI lesion load in monitoring the evolution of multiple sclerosis. Brain 118:1601–1612.

5. Gerig G, Kübler O, Kikinis R, Jolesz FA (1992) Nonlinear Anisotropic Filtering of MRI Data. IEEE Transactions On Medical Imaging 11(2):221–232.

6. Guttmann CRG, Ahn SS, Hsu L, Kikinis R, Jolesz FA (1995) The Evolution of Multiple Sclerosis Lesions on Serial MR. AJNR 16:1481–1491.

7. Kamber M, Collins DL, Shinghal R, Francis GS, Evans AC (1992) Model-based 3D segmentation of multiple sclerosis lesions in dual-echo MRI data. In SPIE Vol. 1808, Visualization in Biomedical Computing pp. 590–600.

8. Kikinis R, Shenton ME, Gerig G, Martin J, Anderson M, Metcalf D, Guttmann CRG, McCarley RW, Lorenson WE, Cline H, Jolesz F (1992) Routine Quantitative Analysis of Brain and Cerebrospinal Fluid Spaces with MR Imaging. Journal of Magnetic Resonance Imaging 2:619–629.

9. Miller DH, Barkhof F, Berry I, Kappos L, Scotti G, Thompson AJ (1991) Magnetic resonance imaging in monitoring the treatment of multiple sclerosis: Concerted Action Guidelines. Journal of Neurology, Neurosurgery,and Psychiatry 54:683–688.

10. Mitchell JR, Karlik SJ, Lee DH, Eliasziw M, Rice GP, Fenster A (1996) Quantification of multiple sclerosis lesion volumes in 1.5 and 0.5 T anisotropically filtered and unfiltered MR exams. Medical Physics 23(1):115–126.

11. Mitchell JR, Karlik SJ, Lee DH, Eliasziw M, Rice GP, Fenster A (1996) The variability of manual and computer assisted quantification of multiple sclerosis lesion volumes. Medical Physics 23(1):85–97.

12. Mitchell JR, Karlik SJ, Lee DH, Fenster A (1994) Classification and Analysis of Multiple Sclerosis Lesions in Spin-Echo MR Exams. In SPIE Vol. 2359, Visualization in Biomedical Computing pp. 362–372.

13. Perona P, Malik J (1990) Scale-space and edge detection using anisotropic diffusion. IEEE Transactions On Pattern Analysis and Machine Intelligence 12(7):629–639.

14. Poggio T, Torre V, Koch C (1985) Computational vision and regularization theory. Nature 317(26):314–319.

15. Schmidt M, Dengler J (1989) Adapting Multi-Grid Methods to the Class of Elliptic Partial Differential Equation Appearing in the Estimation of Displacement Vector Fields. In V Cantoni, R Creutzburg, S Levialdi, H Wolf (eds.), Recent Issues in Pattern Analysis and Recognition, Lecture Notes in Computer Science 399. Springer, Berlin-Heidelberg-New York-Tokyo pp. 266–274.

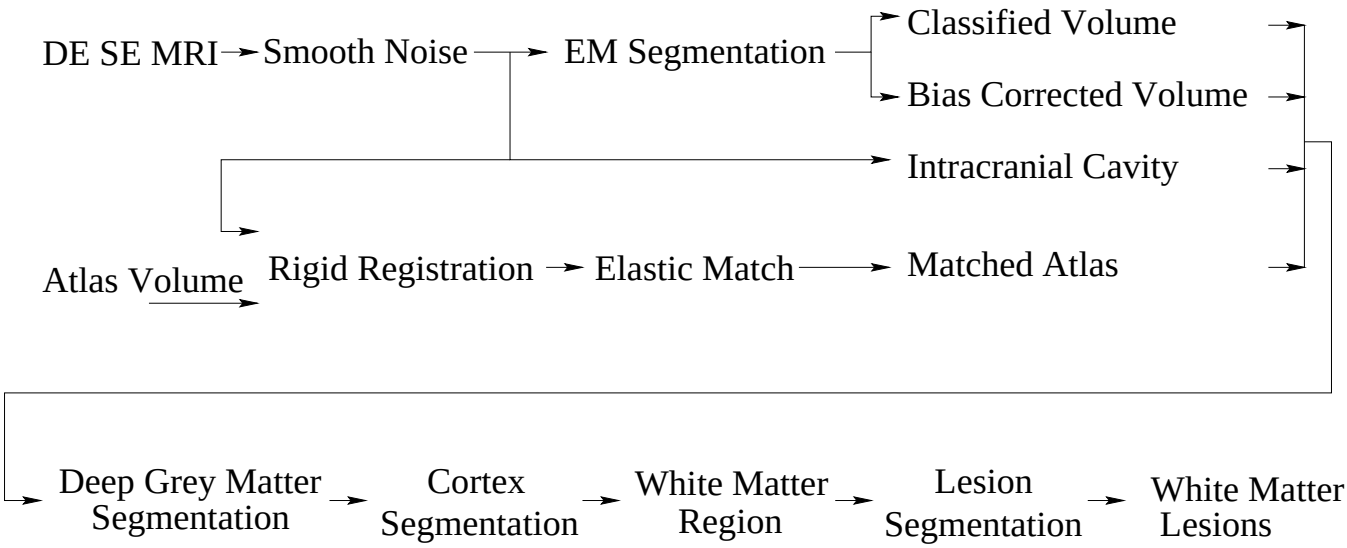

Figure 1: Grey Matter and Lesion Segmentation Scheme

16. Shenton M, Kikinis R, McCarley R, Saiviroonporn P, Hokama H, Robatino A, Metcalf D, Wible C, Portas C, Iosifescu D, Donnino R, Goldstein J, Jolesz F (1995) Harvard Brain Atlas: A Teaching and Visualization Tool. In M Loew, N Gershon (eds.), Proceedings Biomedical Visualization. IEEE Computer Society Press pp. 10–17.

17. Wells III WM, Grimson WEL, Kikinis R, Jolesz FA (1994) Statistical intensity correction and segmentation of MRI data. In SPIE Vol. 2359, Visualization in Biomedical Computing pp. 13–24.

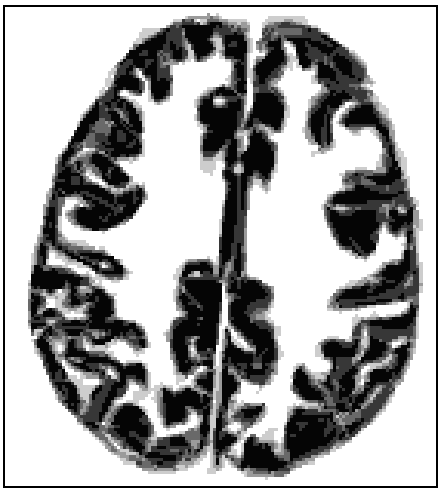

(a) Sum of rater segmentations

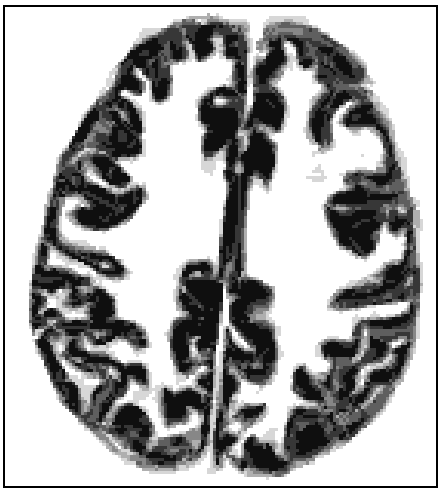

(b) Sum of all segmentations

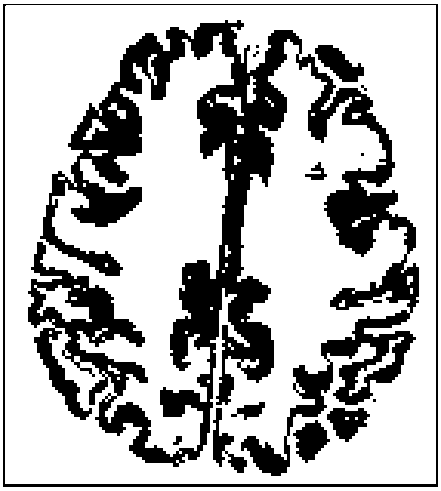

(c) Automatic segmentation

(d) Cortex from elastic match

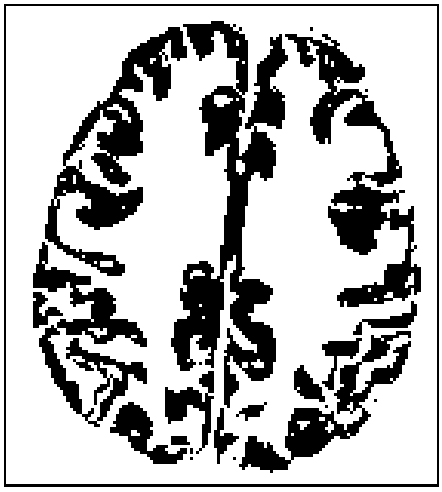

(e) “Standard” cortex segmentation

(f) “Standard” segmentation boundary overlayed on early echo

Figure 2: Cortex segmentation.

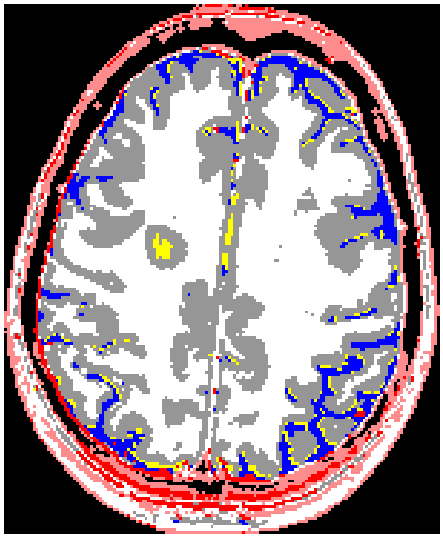

(a) Away from cortex: EM segmenter

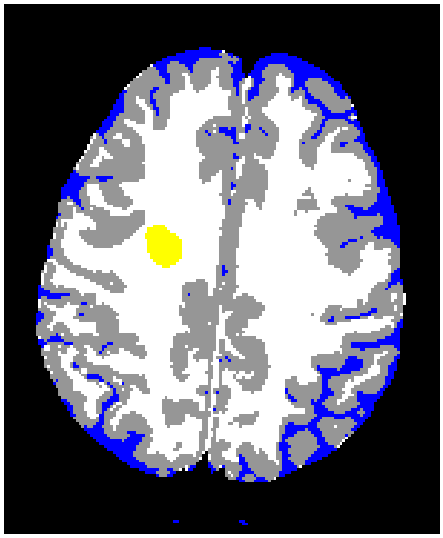

(b) Away from cortex: New method

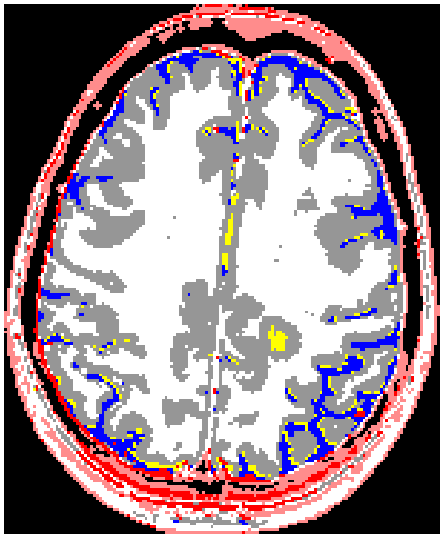

(c) Nearby cortex: EM segmenter

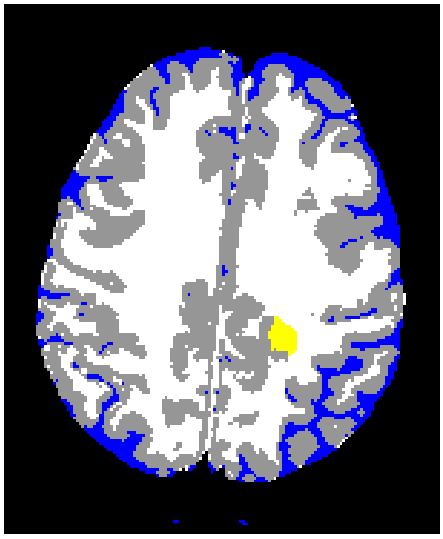

(d) Nearby cortex: New method

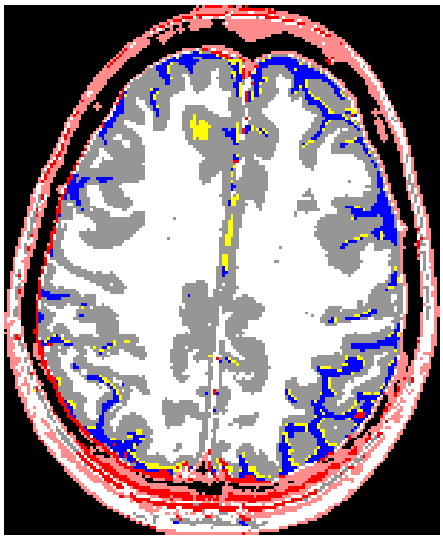

(e) Inside cortex: EM segmenter

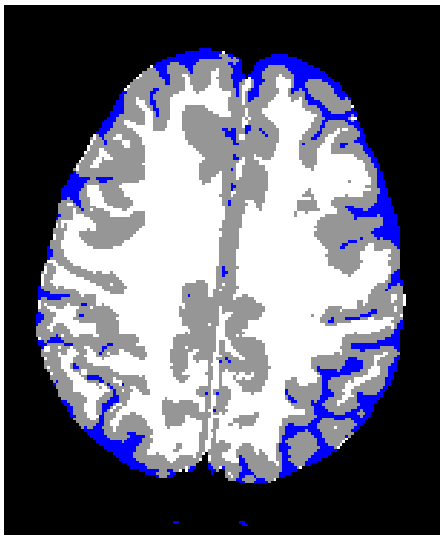

(f) Inside cortex: New method

Figure 3: Illustration of lesion segmentation with EM segmenter and new method.

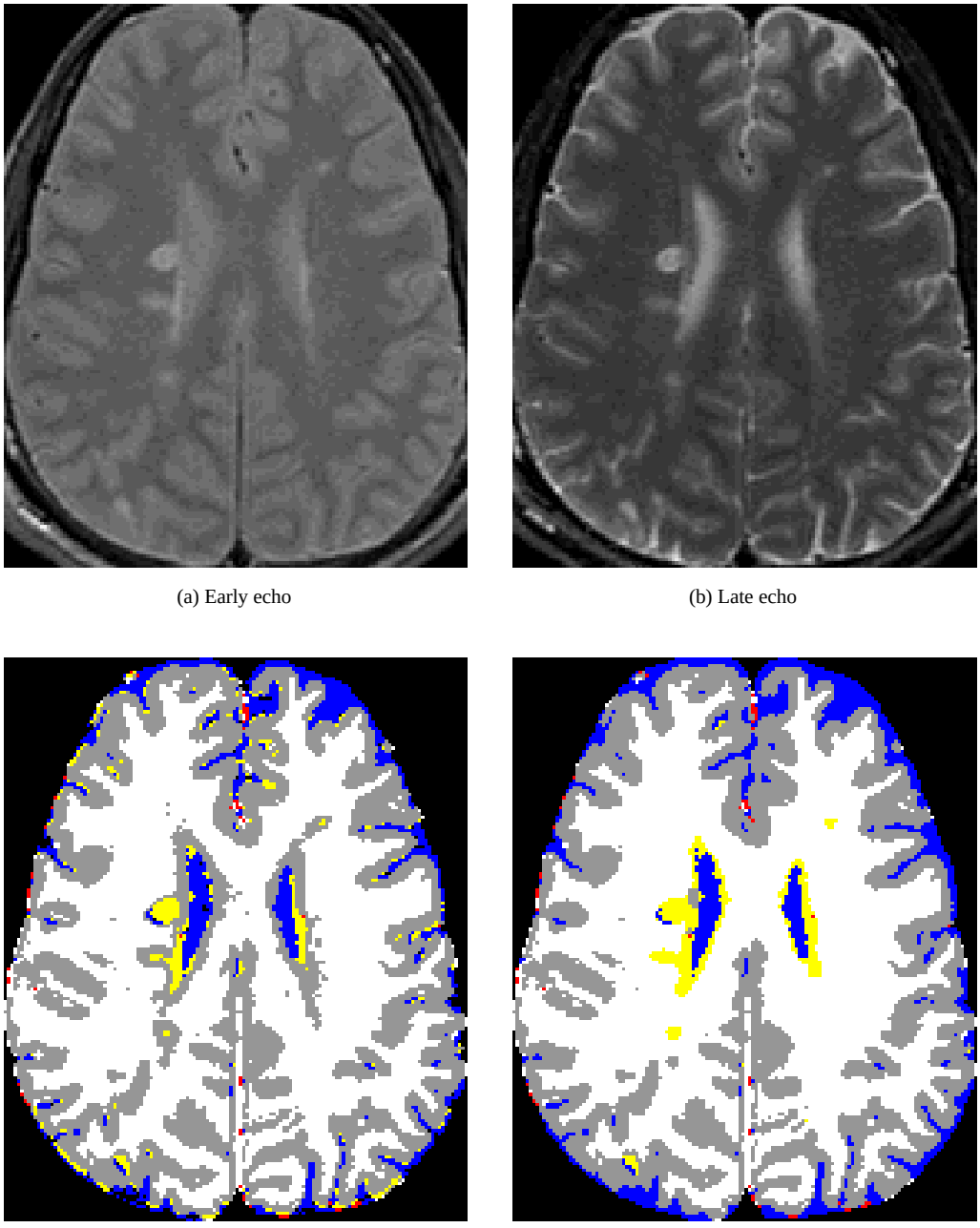

(a) Early echo

(b) Late echo

(c) EM segmenter

(d) New method

Figure 4: Segmentation of white matter, grey matter and white matter lesion: The top row shows the early and late echo images, the bottom row shows the segmentation with statistical classification and with our new algorithm.

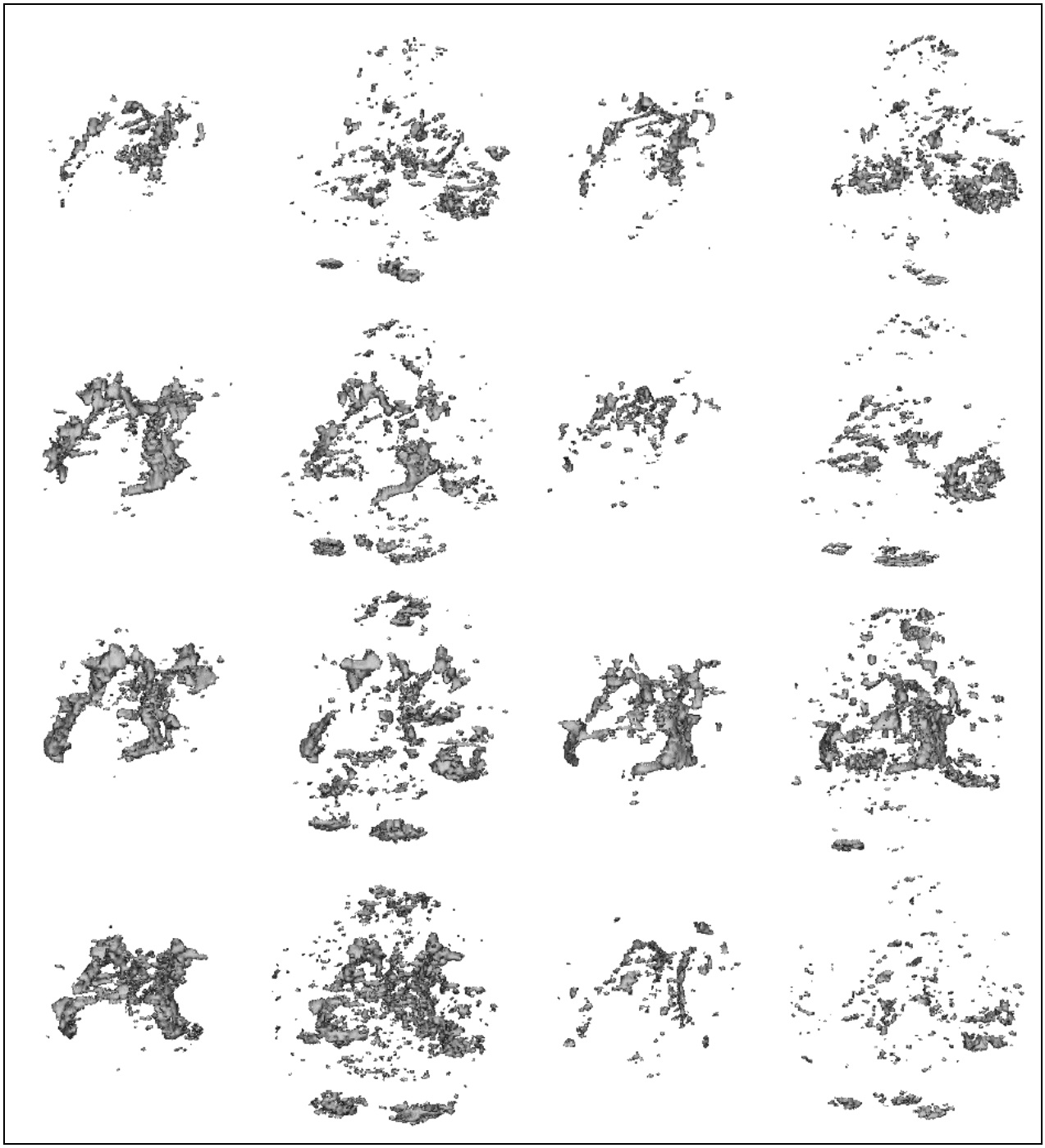

Figure 5: Visualization of segmentation of lesions using the new algorithm (columns 1,3) and the EM segmenter (columns 2,4).

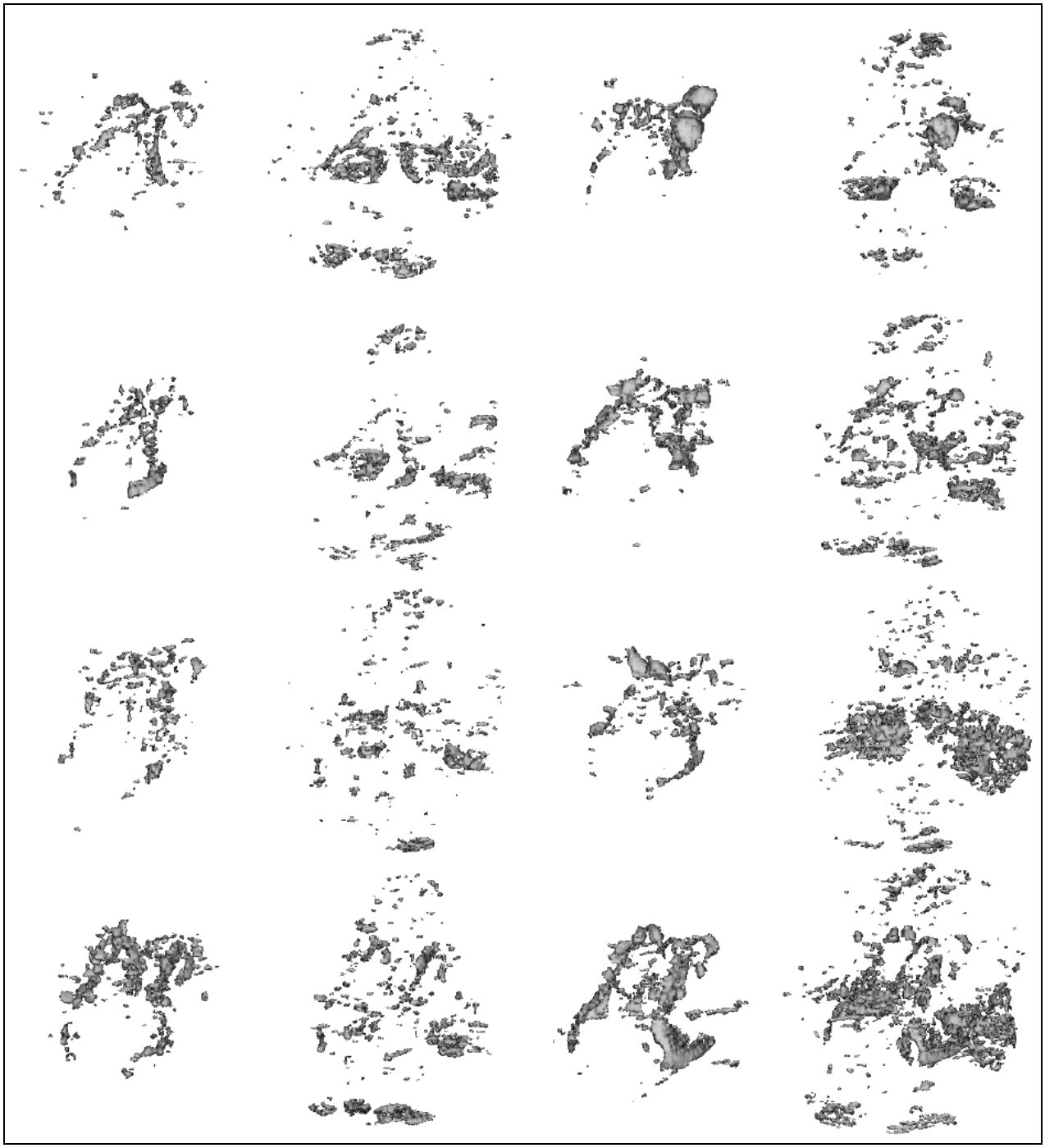

Figure 6: Visualization of segmentation of lesions using the new algorithm (columns 1,3) and the EM segmenter (columns 2,4).

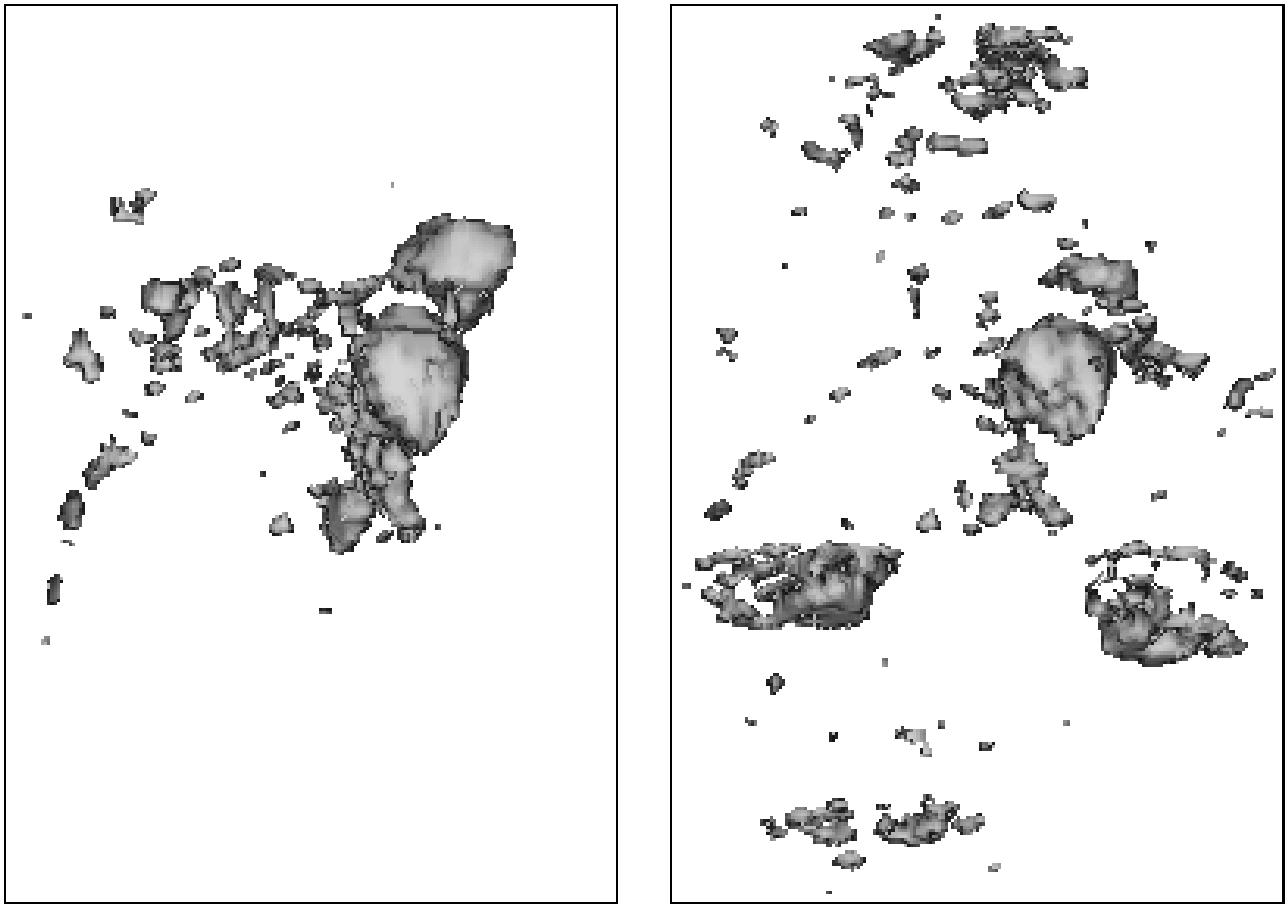

(a) New Method

(b) EM segmenter

Figure 7: Magnified view of images three and four from row one of figure six, showing the segmentation of WML with the new method and the EM segmenter.